Journal of Applied Polymer Science

Surface-Modified Pliable PDLLA/PCL/β-TCP Scaffolds as a Promising Delivery System for Bone Regeneration

Yuanyuan Hu,[1] Jing Wang,[1] Wanli Xing,[1] Lingyan Cao,[1] Changsheng Liu[1,2,3]

[1]Engineering Research Center for Biomedical Materials of Ministry of Education, East China University of Science and Technology, Shanghai 200237, People's Republic of China

[2]The State Key Laboratory of Bioreactor Engineering, East China University of Science and Technology, Shanghai 200237, People's Republic of China

[3]Key Laboratory for Ultrafine Materials of Ministry of Education, East China University of Science and Technology, Shanghai 200237, People's Republic of China

Correspondence to: J. Wang (E-mail: biomatwj@163.com) and C. Liu (E-mail: csliu@sh163.net)

ABSTRACT: Surface-modified poly(D, L-lactide)/polycaprolactone/β-tricalcium phosphate complex scaffold was fabricated in this study and we hypothesized that pliable and mechanical strong scaffold would be achieved by regulation of ternary compositions; while superficial modification strategy conduced to preserve and controlled-release of bioactive growth factors. Properties of the composite scaffolds were systematically investigated, including mechanical properties, surface morphology, porosity, wettability, and releasing behavior. Moreover, the representative cytokine, recombinant human bone morphogenetic protein-2 (rhBMP-2), was loaded and implanted into muscular pouch of mouse to assess bone formation *in vivo*. Improved osteogenesis was achieved ascribed to both amplified β-tricalcium phosphate (β-TCP) content and retarded initial burst release. Particularly, scaffold doped with hydroxypropyl methylcellulose (HPMC) displayed optimal osteogenic capability. The results indicated that the PDLLA/PCL/β-TCP complex scaffold along with HPMC-coating and rhBMP-2 loading was a promising candidate for bone regeneration. © 2014 Wiley Periodicals, Inc. J. Appl. Polym. Sci. **2014**, *131*, 40951.

KEYWORDS: biocompatibility; biomaterials; biomedical applications; composites; drug delivery systems

Received 29 January 2014; accepted 1 May 2014

DOI: 10.1002/app.40951

INTRODUCTION

Nowadays, the number of patients suffering from orthopedic diseases is rapidly increasing, most of them requiring bone grafting for healing. As the limitations of autologous bone grafting are proverbial, an ideal artificial substitute with good biocompatibility and capable of rapid bone formation is accepted. Various bone graft substitutes currently on the market have been met with limited success; however, an area with considerable promise is the growth factors of bone morphogenetic proteins (BMPs).[1] As a member of the transforming growth factor-β (TGF-β) superfamily, the safety and high efficient ossification activity were confirmed by more and more experiments since it was first discovered by Professor Urist in 1963. After continuous research for nearly 50 years, recombinant human BMP-2 (rhBMP-2) has been approved by the US Food and Drug administration (FDA) with an absorbable collagen sponge (INFUSE® Bone Graft, Medtronic) for the treatment of posterior-lateral spine, tibia, and specific craniofacial bone diseases.[2,3]

However, despite its excellent result of bone formation,[4–6] many concerns still exist for its short biological half-life, rapid local clearance, and propensity for side effects.[7] Delivery systems that minimize rapidly diffusion and enzymolysis are desirable not only to enhance bone formation, but also to limit unwanted pathologies.[2] Thus continued research has focused on the optimization of carriers for both structural supports and delivery efficacy to the region of interest.[8]

At present, inorganic materials, synthetic or natural polymers, as well as composites were studied as BMP-2 vehicles. Applications of inorganic materials such as tricalcium phosphate (TCP), hydroxyapatite (HAP), or TCP/HAP porous ceramics are always limited by their brittleness and difficulties in cutting them into desired shapes after forming. Aliphatic polyesters such as polyglycolide (PGA), polylactic acid (PLA), poly (hydroxybutyrate) (PHB), and polycaprolactone (PCL) have attracted much attention because of their biodegradation *in vivo*, nontoxicity of degradation products and variable mechanical strength.[9] But hydrophobic performance of these polymers

weakens their cellular affinity and is undesirable for them to carry water soluble cytokines including rhBMP-2. Except for the physicochemical properties, controlled release of rhBMP-2 is crucial for efficient bone regeneration. Latest research demonstrated that the release behavior was related to the type of BMP-2, non-glycosylated BMP-2 showed slower release from a CaP-based implant compared to glycosylated BMP-2.[5] Moreover, moderate and sustained release rate are optimal for bone healing.[10] Yet, for the sake of its bioactivity, BMP-2 was often adsorbed after the scaffolds were fabricated; it produced some free BMP-2 located on surfaces, which might lead to high initial burst. It could cause a lower BMP-2 amount at therapeutic target than necessary because of rapid initial burst.

Herein we present a kind of delivery system which has good mechanical strength, suits for carrying rhBMP-2, and is easy to be cut into desirable shapes after forming. Since single composition may be not suitable for the complicated requirements of biomedical application,[11] biodegradable PDLLA/PCL/β-TCP complex scaffolds were fabricated. There into β-TCP, a biocompatible calcium phosphate which occurs naturally in the human body and has a chemical composition that corresponds to the inorganic phase of bone,[12–14] was incorporated, acting as a bone filler to endow hydrophilism and osteoconductive.[15,16] Besides, β-TCP also improves the strength of scaffolds. As a result, the porous PDLLA/PCL/β-TCP hybrids fabricated in our work are mechanically stable, moldable, and their mechanical properties can be regulated easily through regulating the ternary compositions.

In addition, to reduce the bolus release originated from the free rhBMP-2 scattering on surfaces, we take advantage of the surface-modification tactics utilizing two kinds of cellulose derivates, sodium carboxymethyl cellulose (CMC), and hydroxypropyl methylcellulose (HPMC), as coatings. Both cellulose polysaccharides are widely used as medicament excipients, which are characteristics of excellent film-forming performance.[17,18] By comparison, scaffolds coated with HPMC have a moderate release rate of rhBMP-2 and display the best ectopic bone formation. Thus, we hypothesize that the PDLLA/PCL/β-TCP scaffold along with HPMC coating is a promising delivery system of rhBMP-2 in applications of bone tissue engineering. To our knowledge, there has not been a systematic investigation of surface-modified porous PDLLA/PCL/β-TCP hybrid scaffolds, and there is no report about its application as an rhBMP-2 carrier for bone regeneration either.

EXPERIMENTAL

Materials

Poly-D-L-lactide (PDLLA, M_η = 300 KD) and polycaprolactone (PCL, M_η = 150 KD) were purchased from Jinan Daigang Biomaterial (Shandong, China). HPMC was purchased from Shandong Liaocheng A Hua Pharmaceutical (Shandong, China). CMC was obtained from Shanghai Chineway Pharmaceutical Tech (Shanghai, China). β-TCP was prepared in laboratory. Recombinant human bone morphogenetic protein-2 (rhBMP-2) was generously provided by Shanghai Rui Bang (Shanghai, China). All other solvents were of analytical grade and used without further purification.

Fabrication of Porous PDLLA/PCL/β-TCP Scaffolds

Porous PDLLA/PCL/β-TCP scaffolds were obtained by a salt particulate leaching method combining polymer coagulation and cold compression molding. Specifically, β-TCP powders were dispersed into dichloromethane primarily, then PDLLA and PCL were added into the dichloromethane which contained β-TCP, subsequently vigorous stirring was conducted to form a well distributed mixture. After that, sieved NaCl particles ranging from 300 μm to 500 μm were dispersed uniformly into the mixture by a homogenizer. The thick PDLLA/PCL/β-TCP/NaCl mixture was then filled into a rectangular prism mould of 80 $\times$ 10 $\times$ 4 mm in overall dimensions and a cylindrical mould of 10 mm in diameter and compressed under pressures for one minute at room temperature. After vacuuming at 37°C for 24 h, the molded composites were put into distilled water for a period of 2–3 days for salt leaching; the water was refreshed every 2 h during the first 10 h and then 2–3 times a day. When there was no white precipitate detected after dripping silver nitrate solution into the water, the samples were taken out and vacuum dried to obtain the cylindrical and rectangular prism porous PDLLA/PCL/β-TCP scaffolds. The composition variation of PDLLA/PCL/TCP were as follows:

$$\text{PDLLA}/\text{PCL}(100:0;75:25;50:50;25:75;0:100\text{w}/\text{w});$$

$$\text{PDLLA}/\text{PCL}/\beta-\text{TCP}(40:40:20;30:30:40\text{w}/\text{w}/\text{w}).$$

Surface-Modified Procedure

The CMC and HPMC solutions were prepared by dissolving a certain amount of CMC (1%, g/mL) and HPMC (2%, g/mL) in ultrapure water and stirring until the transparent solutions were obtained. Dripping the two kinds of solutions onto surfaces respectively until scaffolds were totally encapsulated, afterwards drying the scaffolds at 37°C for 48 h. The ratio of solution/scaffold is about 4:1 (mL/g).

Preparation of rhBMP-2-Loaded Scaffolds

Processing was conducted in sterile conditions. The scaffolds were sterilized by ethylene oxide; and the CMC solution (1% g/mL) and HPMC solution (2% g/mL) were sterilized by filtration. Then the rhBMP-2 (0.5 mg/mL) aqueous solution was dripped onto the porous scaffolds. The ratio of rhBMP-2/scaffold is about 2 : 1(μL/mg). After lyophilization, the rhBMP-2-loaded scaffolds were produced. As for the rhBMP-2-loaded surface-modified scaffold, similar incipient steps were conducted. Before lyophilization, dripping the CMC solution (1%, g/mL) or HPMC solution (2%, g/mL) onto the BMP-2-loaded scaffolds uniformly, and then freeze-dried.

Mechanical Properties

Three point bending test for rectangular prism samples (80 $\times$ 10 $\times$ 4 mm) and compression test for cylindrical samples (10 mm in diameter and 20 mm in height) were both performed at a loading rate of 2 mm/min using a universal testing machine (HY-0230, China). Bending modulus and compression modulus were calculated by the initial slopes of relevant stress–strain curves. Three replicates were carried out for each group, and the results were expressed as mean $\pm$ standard deviation (mean $\pm$ SD).

Morphology Investigation

Scanning electron microscopy (JSM-6360LV, Japan) was used to observe the morphology of the porous PDLLA/PCL/β-TCP

scaffolds surfaces before and after the CMC or HPMC coating. To improve conductivity, the gold sputter was used.

Porosity Measurement

The open porosity can be calculated by the liquid displacement method.[19] The scaffold was submerged in a known volume (V_1) of ethanol and a series of brief evacuation repressurization cycles were conducted to force the liquid into the pores of the scaffold. After these cycles the volume of the liquid and liquid-impregnated scaffold was V_2. When the liquid-impregnated scaffold was removed, the remaining liquid volume was V_3 and open porosity was given as: $\Pi = (V_1 - V_3)/(V_2 - V_3)$. Three replicates were carried out for each kind of scaffold fabricated in this study.

Water Contact Angle Measurements

Water contact angle measurement was undertaken to evaluate the effect of different β-TCP weight ratios on the surface hydrophilicity of PDLLA/PCL samples. CMC- or HPMC-coated samples were also studied. To eliminate the deviation made by porous surfaces of scaffolds, all the samples were made into films. Concisely, PDLLA/PCL/β-TCP complex films were prepared by dissolving the ternary composition in dichloromethane and stirring vigorously to form a well-distributed mixture, subsequently volatilizing dichloromethane completely at room temperature, then film samples were obtained. CMC- or HPMC-coated films were produced just like porous scaffolds which mentioned above. The water-in-air contact angle of the film was measured by contact angle meter (JC2000D3, China). The film was placed onto the work stage of the meter. The contact angle was measured within 10 s after a droplet of distilled water (5 μL) contacted the film surface. Five replicates were carried out for each group.

Zeta Potential

The interactions between rhBMP-2 and CMC or HPMC were determined in solutions by zeta potential method (Nicomp 380 ZLS, America). According to the zeta potential, the acting force between rhBMP-2 and CMC or HPMC is attractive or repulsive could be clear.

In Vitro Release Study

RhBMP-2-loaded porous scaffold was placed in a closed vial containing 10 mL of phosphate buffered saline solution (PBS, pH = 7.4), and kept in a concussion incubator at 37°C for 35 days. The release medium was collected at different point-in-time (1, 2, 3, 5, 7, 14, 21, 28, 35 days), and replaced with the same volume of fresh PBS. The sample mediums were analyzed by ELIASA (SPECTRA max PLUS384); the effects of β-TCP weight ratios and surface-coatings on release behavior of rhBMP-2 were studied. All experiments were performed in triplicate for each sample.

Cytotoxicity Assay

Cytotoxicity of porous scaffolds was determined using MC3T3-E1 cell by the 3-(4, 5-Dimethylthiazol-2-yl)−2, 5-diphenyltetrazolium bromide (MTT) method. Murine preosteoblastic MC3T3-E1 cells derived from mouse calvarium tissue and obtained from the American Type Culture Collection (ATCC) were cultured in complete medium containing α-minimal essential medium (α-MEM, GIBCO, Grand Island, NY), supplemented with 10% fetal bovine serum (FBS, Sijiqing, Hangzhou, China), 1 mM sodium pyruvate, 2 mM L-glutamine, 100 U/mL penicillin, and 100 μg/mL streptomycin in a humidified atmosphere with 5% CO_2 in air at 37°C.

Put scaffolds ($d = 10$ mm, $h = 1$ mm) into 24-well plates, then cells at a density of 1.0×10^4 cells a well were seeded. After incubation in a humidified 5% CO_2 incubator (RCO3000T-5-VBC) at 37°C for 24 h and 72 h, 100 μL of MTT solution (5 mg/mL) was added to each well and incubated for an additional 4 h. The medium was then aspirated from the wells and 1 mL of dimethyl sulfoxide (DMSO) was added to each well for dissolving the formazan products and the absorbance was measured at 490 nm using ELIASA (SPECTRA max PLUS384). The blank group (cells in medium only) acted as the negative control. Five replicates were carried out for each group. The percentage of viability was expressed as the relative growth rate (RGR) as follows:

$$\mathrm{RGR} = \mathrm{OD}_t / \mathrm{OD}_{\mathrm{nc}} (\%)$$

where OD_t and OD_{nc} are the optical density of tested sample and the negative control, respectively.

Ectopic Bone Formation

The experiment was approved by the Animal Experimentation Ethics Committee. 40 Kunming male rats (body weight 23–25 mg) were used in this operation. They were randomly divided into five groups. All surgical procedures were carried out under sterile conditions. General anaesthesia was induced using intramuscular injections of 3% sodium-pentobarbital (40 mg/Kg). The inner leg of each rat was shaved and scrubbed with 75% ethanol for disinfecting. After incision of the skin, five groups of samples were implanted into the hind limbs of rats (one implant per animal). Closure of the skin was conducted with degradable suture. Post-operatively, standard diet was supplied.

Animals were sacrificed at scheduled time to evaluate the ectopic bone formation. Three specimens of each group were pulled off and the wet weight and ash contains (calcined at 600°C in muffle furnace for 4 h) of the ectopic formed bone were obtain at reserved time point of 2 and 4 weeks. The rest harvested bony specimens with surrounding tissues were excised and assigned to histological analysis. After fixation with 4% neutral buffered formalin for 24 h, the extracted bones were decalcified in 12.5% EDTA, dehydrated in gradients of alcohol, and paraffin-embedded. Serial sections were stained using hematoxylin/eosin (HE) and masson trichrome staining method and observed under a light microscope (Nikon TE2000U, Japan).

Statistical Analysis

Values are reported as mean ± SD. Coupled data sets were compared by Student's t test. Statistical significance was accepted at values of $P < 0.05$.

RESULTS AND DISCUSSION

Mechanical Properties of Porous Scaffolds

The three essential elements for bone tissue engineering are osteoconduction, osteoinduction, and osteogenesis. In bone

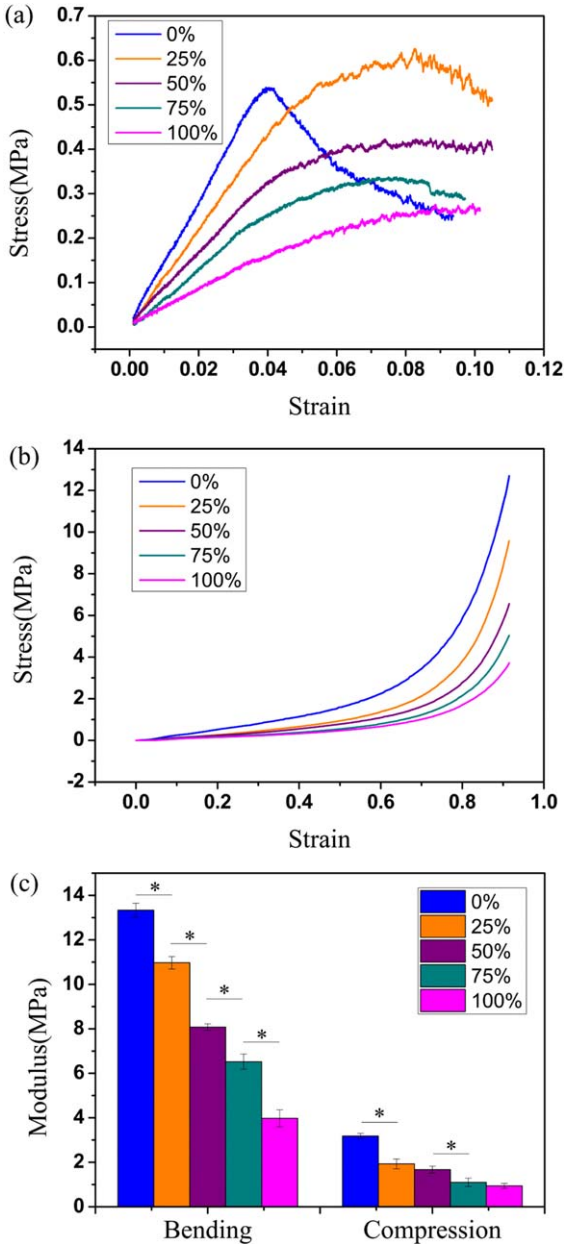

Figure 1. Typical mechanical properties of PDLLA/PCL porous scaffolds with various mass fraction of PCL. (a) Bending stress–strain curves; (b) compressive stress–strain curves; (c) bending and compression modulus of PDLLA/PCL scaffolds with different PCL content (*$P < 0.05$). [Color figure can be viewed in the online issue, which is available at wileyonlinelibrary.com.]

healing procedures, artificial implants performed as osteoconductive materials were limited by several methodological disadvantages that consist of non-physiological nature of the materials, the pathogen transmission, the toxic nature of degradation products, the brittleness of materials, and the difficulty in preparation.[20] The use of engineered porous polymer scaffolds as structural bone substitutes offers promising properties overcome these disadvantages. The mechanical response of polymers is characterized as a competition between elastic and plastic deformation and one promising method for tuning material properties is complex. In our study, PDLLA/PCL porous scaffolds with various PCL content (0%, 25%, 50%, 75%, and 100%, w/w) were fabricated successfully, and their mechanical properties were investigated by bending and compression tests. The bending stress-strain curves of PDLLA/PCL blends in Figure 1(a) showed that the pure PDLLA porous scaffolds were broken under a low stress, while PDLLA/PCL scaffolds displayed increased strain under a same stress by the increased PCL content, which claimed scaffolds with higher PCL content were softer than the scaffolds with lower PCL content. It was reinforced in Figure 1(b), demonstrating increased strain under the same stress in the compression test as the PCL content amplified. Figure 1(c) showed the bending and compression modulus with the variation of PCL percent. With the increment of PCL, both modulus decreased, and distinct differences of bending modulus between every two adjacent groups could be seen, while the differences of compression modulus were not so distinct. On the basis of mechanical test, PDLLA and PCL are complementary in mechanical properties. Flexibility of porous PDLLA increased when PCL incorporated mainly because of the softness of PCL. On the contrary, the rigid property of PDLLA strengthened PCL. Not the best but moderate ratio of 50:50 (PDLLA/PCL) was chosen for subsequent investigations.

Scaffolds A, B, and C which enumerated in Table I were fabricated to investigate the influences of β-TCP content on PDLLA/PCL scaffolds' performance while scaffolds D and E were produced to study the effects of superficial coatings. The influence of β-TCP content on the toughness and strength is displayed in Figure 2(a). As the ratio of β-TCP content increased the scaffolds indicated lower strain under the same stress which claimed a stronger property in bending test. What's more important, the scaffolds were not broken with the increasing β-TCP content, that is to say, scaffolds did not become brittle due to the inorganic particles and the pliable and flexile properties reserved. This conclusion can be reinforced in Figure 2(b), demonstrating decreased strain under the same stress in the compression test as the β-TCP content amplified. Figure 2(c) showed the compression and bending modulus with the variation of β-TCP portion, with the increment of β-TCP, both kinds of modulus increased.

Scaffolds containing 40% β-TCP were selected to investigate effects of surface-coating with CMC or HPMC. Figure 2(c) indicated both coatings successfully improve the bending and compression modulus, meanwhile, the flexibility is remained. For a comparison, modulus of HPMC-coated scaffolds is higher than that of CMC-coated scaffolds. The pliable and strong porous scaffolds were beneficial for bone regeneration.

Figure 3 showed the representative moldable property of PDLLA/PCL/β-TCP scaffolds of group C. The pliable strip scaffold did not fracture under a large deformation, and it could recover nearly to the original shape spontaneously and immediately. The cylindrical scaffold was also not broken after compression; there was just a decrease in the height compared with the original one.

Microstructure Observation

PDLLA/PCL blends in a wide composition range have been studied for many years, the immiscibility of PDLLA and PCL

Table I. Porosity and Contact Angle of PDLLA/PCL/β-TCP Scaffolds

Group	Composite	Porosity (%)	Contact angle (°)
A	PDLLA/PCL (50:50,w/w)	84.45	103.32 ± 4.50
B	PDLLA/PCL/β-TCP (40:40:20,w/w/w)	82.01	72.33 ± 3.93
C	PDLLA/PCL/β-TCP (30:30:40,w/w/w)	80.77	63.90 ± 3.17
D	PDLLA/PCL/β-TCP (30:30:40,w/w/w) + CMC	69.12	49.94 ± 4.36
E	PDLLA/PCL/β-TCPC (30:30:40,w/w/w) + HPMC	53.49	47.64 ± 2.54

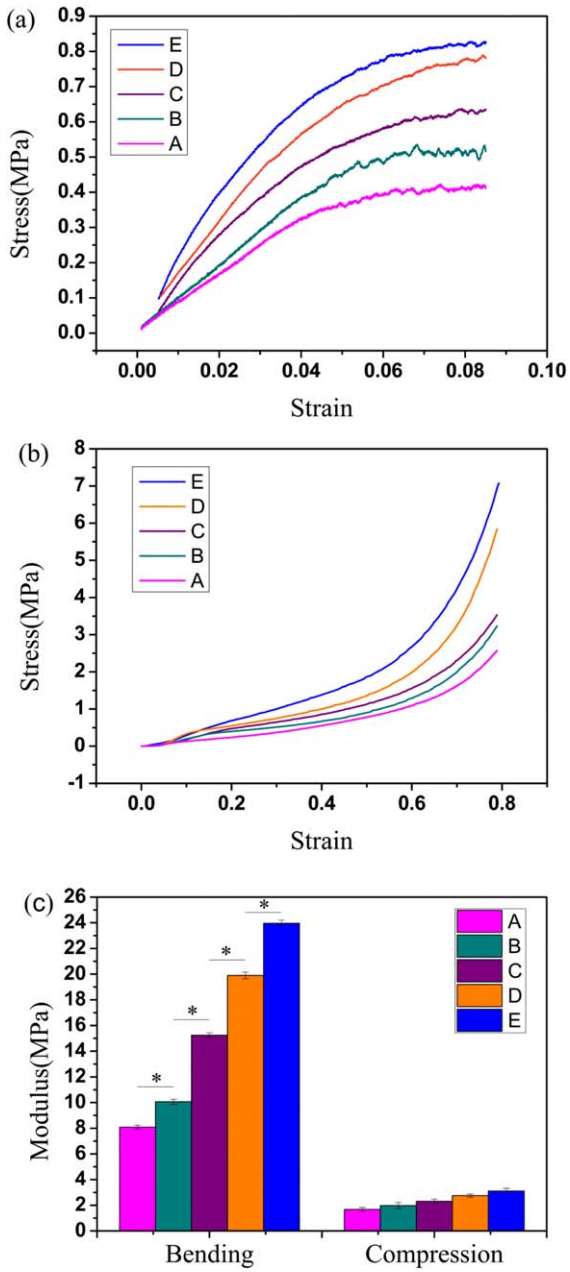

Figure 2. Typical mechanical properties of five groups of composite scaffolds. (a) Bending stress–strain curves; (b) compression stress–strain curves; (c) bending and compression modulus of scaffolds with different β-TCP content and various superficial modifications (*$P < 0.05$). [Color figure can be viewed in the online issue, which is available at wileyonlinelibrary.com.]

has been reported, [21] however in this article, SEM micrographs of PDLLA/PCL scaffolds in Figure 4(a–c) do not show a distinct two phases morphology with particles dispersed in a matrix in accord with Dinorah Newman's research,[22] PDLLA/PCL blends present a certain degree of miscibility. He explained it as the effect of the addition of PCL chains to the amorphous PDLLA phase, which renders an existing rigid amorphous phase mobile, allowing the chain folding and the cooperative motions possible in this phase.

It was clearly seen that the pores of PDLLA/PCL scaffolds were distributed homogeneously with pore size range from 200 to 500 μm and the pore walls were quite flat in Figure 4(a–c). As showed in Figure 4(d–f), the pores became irregular and rough with incorporation of β-TCP, and β-TCP nano particles were obviously seen in the pore walls. Specifically, with the increment of β-TCP content, more irregular pores were observed, and more β-TCP nano particles visibly distributed in pore walls in Figure 4(g–i). The pore size and interconnectivity did not

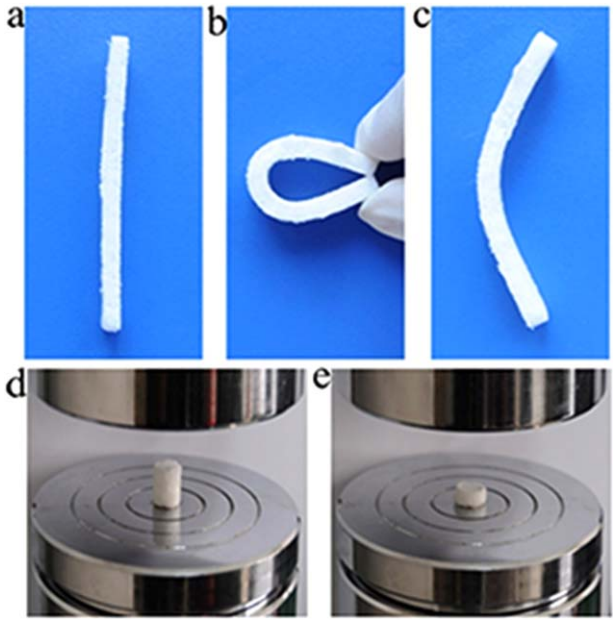

Figure 3. Representative moldable PDLLA/PCL/β-TCP scaffolds (group C). (a) Original strip scaffold; (b) bending scaffold with hands; (c) spontaneous recovery of scaffolds after deformation; (d) original cylindrical scaffold before compression; (e) compressed cylindrical scaffold. [Color figure can be viewed in the online issue, which is available at wileyonlinelibrary.com.]

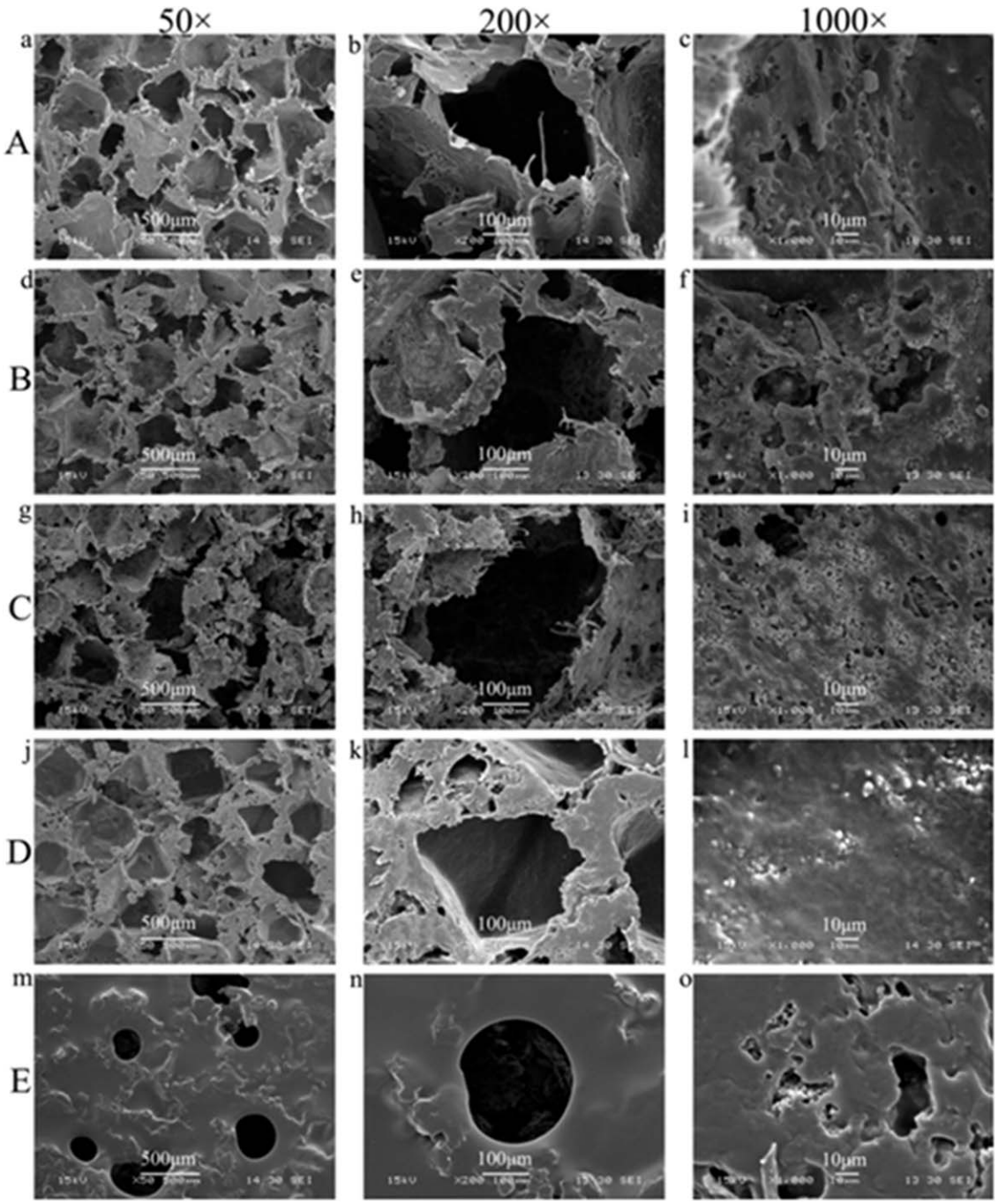

Figure 4. SEM graphs of scaffolds with various prescriptions. Original magnification: left column 50×; middle column 200×; right column 1000×. Group A–E were described in Table I.

change much with the incorporation of β-TCP. The interconnectivity of the scaffolds is noteworthy for it is necessary to promote cell growth, cell migration and the transport of nutrients and oxygen, as well as the removal of metabolic waste. As a bone scaffolds, a minimum requirement of 100 μm for the pore size was suggested by Karageorgiou.[23] It is observed in SEM micrographs, the pore size ranged from 200 to 500 μm, which was close to those of the sieved NaCl particle size, meeting the minimum requirement of the pore size for a bone scaffold. Although irregular and rough surfaces were obtained by filling of β-TCP, the loose and interconnected structure which suitable for cell adhesion and nutrition transmission still remained.

Surface morphology of HPMC-coated scaffold was displayed in Figure 4(m–o), the majority of pores were covered and the porous structure were faintly visible through the HPMC coating, and β-TCP nano particles were nearly invisible in pore walls. For a comparison, the initial interconnected porous structure was almost maintained after the CMC coating, though

some small pores were closed. Surface of CMC-coated scaffolds were smoother than the uncoated ones. The outlines of inorganic nano particles covered by CMC in pore walls were still observed in Figure 4(l). Additionally, superficial film forming of HPMC or CMC enhanced the mechanical properties according to the mechanical results. Due to a better film forming property of HPMC compared to CMC which was observed in SEM micrographs (j and m), the increment of modulus owing to HPMC is higher than that of CMC. The surface changes caused by HPMC and CMC coatings are temporary, the original microstructure of scaffolds will be regained after the dissolution of HPMC and CMC.

Porosity

In our study, we found that if polymer/porogen weight ratio was unchangeable, the porosity of PDLLA/PCL scaffolds almost kept steady regardless of PDLLA/PCL ratios (datum not listed in this paper). On the other hand, Table I indicated that, with amplified β-TCP content, the porosity of scaffolds decreasing in a tiny scale. Considerable reductions of porosity attributed to coatings were also observed in Table I. Compared with uncoated scaffolds, the porosity of HPMC-coated scaffolds reduced by nearly 30%, CMC-coated scaffolds reduced by about 10%. Additionally, to our knowledge, highly porous and interconnected structure is required to minimize the amount of polymer and increase the surface area of biodegradable scaffolds for tissue regeneration of damaged tissues. According to Table I, although there is a small reduction in porosity when β-TCP incorporated, the porosities of scaffolds were all above 80% in our work despite of HPMC or CMC coated ones. As for coated scaffolds, the considerate reduction in porosity is temporary, with the dissolution of HPMC and CMC, the original porosity will be regained.

Hydrophilicity Examination

Since the porous surface of scaffold is not suitable for the water contact test, the composite films with flat surfaces were used. It is illustrated in Table I that water contact angle of group A is 103.32°, which indicates the most hydrophobic compared with other groups. In group B and C, with the increment of β-TCP, the water contact angles decrease to 72.33° and 63.90°, respectively, which means the improvement of Hydrophilicity. Obviously, in groups D and E, water contact angles of the composite films coated with CMC or HPMC were much smaller, demonstrating better hydrophilism. Both CMC and HPMC can dissolve in water; it might explain why they can improve the Hydrophilicity of composite film surfaces. Good hydrophilism benefits cell attachment and growth on the surface of materials.

Zeta Potential

According to the results of ζ-potential, BMP-2 (1.05 mV), and β-TCP (27.16 mV) surfaces were positively charged while CMC (−41.92 mV) and HPMC (−1.13 mV) surfaces were negatively charged. As we all know that molecules with opposite charges are attracted to each other.

Release Kinetics of BMP-2 *In Vitro*

Figure 5 illustrated the influence of various β-TCP ratios (0%, 20%, 40%) and the surface coating protocol on release behavior of rhBMP-2. Pure PDLLA/PCL scaffolds showed the fastest BMP-2 release rate. With amplified β-TCP content, the release rate decreased. Despite the small differences, uncoated scaffolds showed similar release profiles. Great cumulative BMP-2 release amount of 85%, 75%, and 70% for three different β-TCP weight ratios of 0%, 20%, and 40%, in the first seven days respectively indicated higher initial burst. And the rest BMP-2 was sustainably diffused out of the scaffolds over the following 28 days. On the other hand comparisons were made not only between the scaffolds with and without coatings, but also between scaffolds with different coatings. In Figure 5, we could see both HPMC- and CMC-coated scaffolds presented lower initial burst than uncoated ones. Cumulative BMP-2 release amount dropped to 50% and 37% in the first 7 days for HPMC and CMC-coated scaffolds, respectively. Thereafter, the release rate was almost constant until the end of observation for both coated scaffolds.

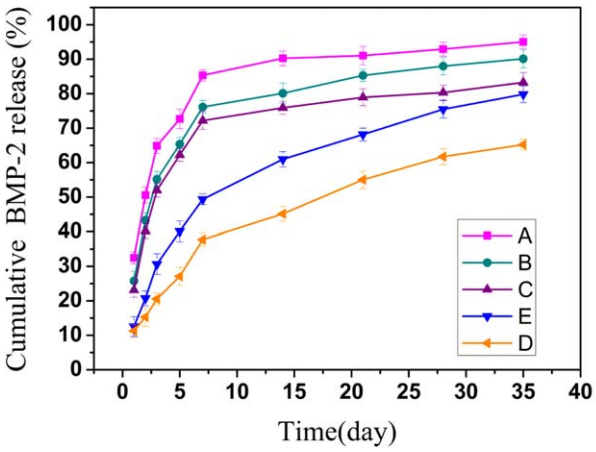

Figure 5. Release profiles of rhBMP-2 for five groups of scaffolds in Table I. [Color figure can be viewed in the online issue, which is available at wileyonlinelibrary.com.]

It is reported that burst followed by sustained release is an optimal release profile of rhBMP-2 in bone regeneration.[24] In Figure 5 all the profiles show an initial burst of BMP-2 release from scaffolds and followed by a slower sustained release. About 70–85% of BMP-2 was released from uncoated scaffolds within 7 days. In BMP-2 loading procedure which mentioned before, BMP-2 solution was dropped onto the scaffolds surfaces, a portion of BMP-2 infiltrated into scaffolds, whereas much BMP-2 still located on the surfaces of scaffolds. Theoretically speaking, free BMP-2 located on surfaces was a principle reason why the burst occur. Among the three uncoated scaffolds (group A, B and C in Table I), with increment of β-TCP, rate of BMP-2 release became slower. It might because the addition of β-TCP improves hydrophilicity of PDLLA/PCL composite scaffolds; better hydrophilicity allows more BMP-2 solution impregnate into porous scaffolds, leading to a smaller percentage of BMP-2 locating on surfaces. Furthermore, rough surfaces originated from introduction of β-TCP are beneficial for BMP-2 adsorption as well. If without any protection measures, losses of BMP-2 during operation procedures would be great. Superficial coating methods is a kind of convenient strategy decreasing the

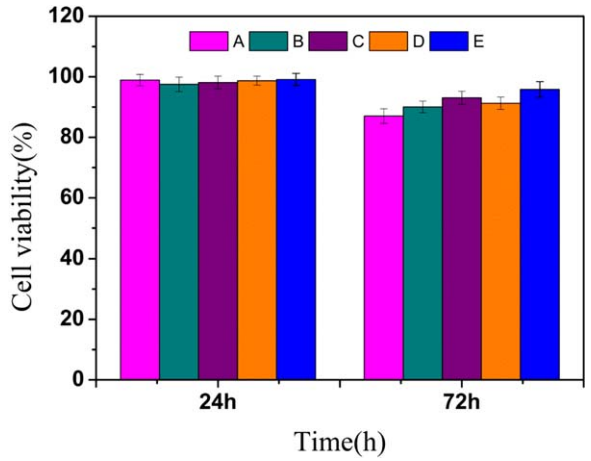

Figure 6. Cytotoxicity of scaffolds by MTT analysis after incubation for 24 h and 72 h. [Color figure can be viewed in the online issue, which is available at wileyonlinelibrary.com.]

initial burst and obtain a gentle release profile from delivery systems.[8,25] It is reported that the consistency and strength of the film formed at the scaffolds surface are crucial factors in determining drug release mechanism and the rate of release from the polymeric system.[26] Encapsulation of BMP-2-loaded scaffolds by CMC or HPMC coatings may reduce this kind of undesirable losses. Furthermore, interactions between rhBMP-2, β-TCP, HPMC, and CMC may influence the effect of encapsulation protections. The zeta-potentials of rhBMP-2 and β-TCP are positive, both CMC and HPMC solutions are negative. Additionally, the zeta-potential of CMC solution is much lower than that of HPMC solution, so a stronger attraction between β-TCP and CMC or between rhBMP-2 and CMC is obtained compared to HPMC, respectively. As a result, CMC films can better attached to β-TCP filled scaffolds surfaces than HPMC films. More than that, as rhBMP-2 could be easily and stably entrapped by the stronger mutual attraction, the rate of rhBMP-2 release from CMC-coated scaffolds might be slower than HPMC coated ones. This hypothesis was confirmed in Figure 5. On the other hand, compared with uncoated scaffolds, CMC or HPMC coated ones both showed lower initial burst and slower release rate. More than that, CMC-coated scaffolds performed the most retarded controlled release for rhBMP-2.

Cell Viability

Figure 6 indicated that viability of MC3T3-E1 cells was little affected by the five groups of scaffolds. The RGR of each group was above 95% after incubated for 24 h, corresponding toxic grade 1 according to ISO 10993–5: 2009, which means all scaffolds are tolerant in cellular application. Little differences can been seen between five groups after incubated for 72h, although pure PDLLA/PCL scaffolds showed the lowest cell viability, the RGR was still above 80%, corresponding toxic grade 1. The β-TCP filled scaffolds indicated improved cell viability compared to unfilled scaffolds. Besides, both CMC- and HPMC-coated scaffolds performed good compatibility with MC3T3-E1 cells.

Ectopic Bone Formation

Wet weight and ash weight of ectopic bone was used to assess the bone formation. According to Figure 7(a) and (b), differences between five groups of scaffolds are distinct. With the increment of β-TCP, both kind of weight increased. Additionally, not only CMC but also HPMC displayed large increment in the weight of newly formed bone, most of all, the HPMC-coated scaffolds showed the optimal osteogenesis.

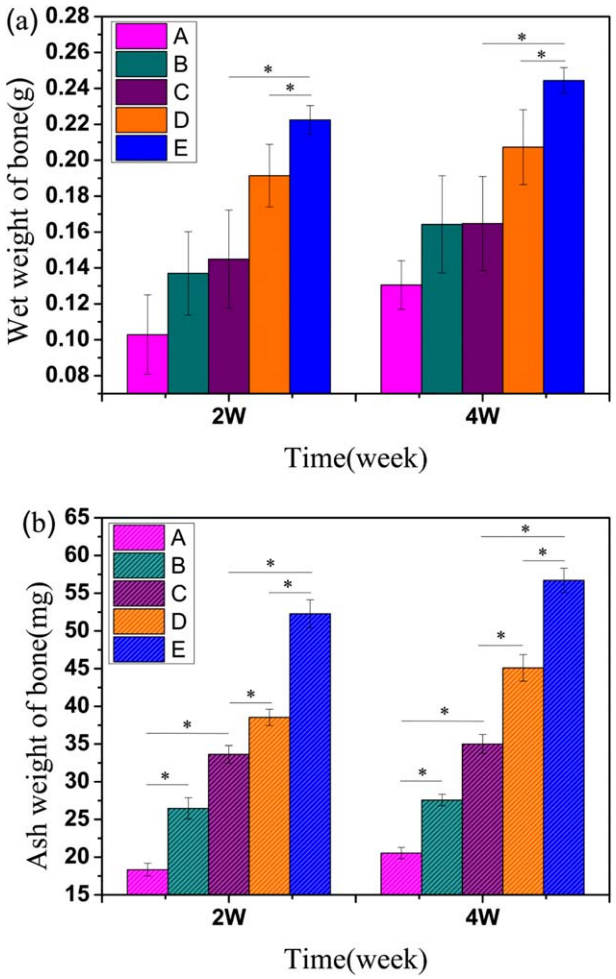

Figure 7. Wet weight (a) and ash weight (b) of new bone for 2 weeks and 4 weeks ($^*P < 0.05$). [Color figure can be viewed in the online issue, which is available at wileyonlinelibrary.com.]

The HE and Masson's trichrome staining methods further consolidated the trend of five groups of scaffolds in newly formed ectopic bone. From Figures 8 and 9, the implants were totally encapsulated by a thin layer of fibrous tissue both at the 2nd and 4th week. For group A, B, and C, at the 2nd week, it was clearly seen that the newly formed bone area and the material area were separated, few osteocytes attached to the scaffolds, large quantity of undegraded materials were observed in both HE and Masson's trichrome staining sections. At 4 weeks, mature trabeculae, less undegraded materials was revealed in HE staining. And more osteocytes were proliferated into material areas in Masson's trichrome staining. Since there were increasing of new bone formation and decreasing of undegraded materials as the increment of β-TCP, the β-TCP-enriched scaffolds performed better osteoconductive and osteoinductive properties than pure PDLLA/PCL scaffolds.

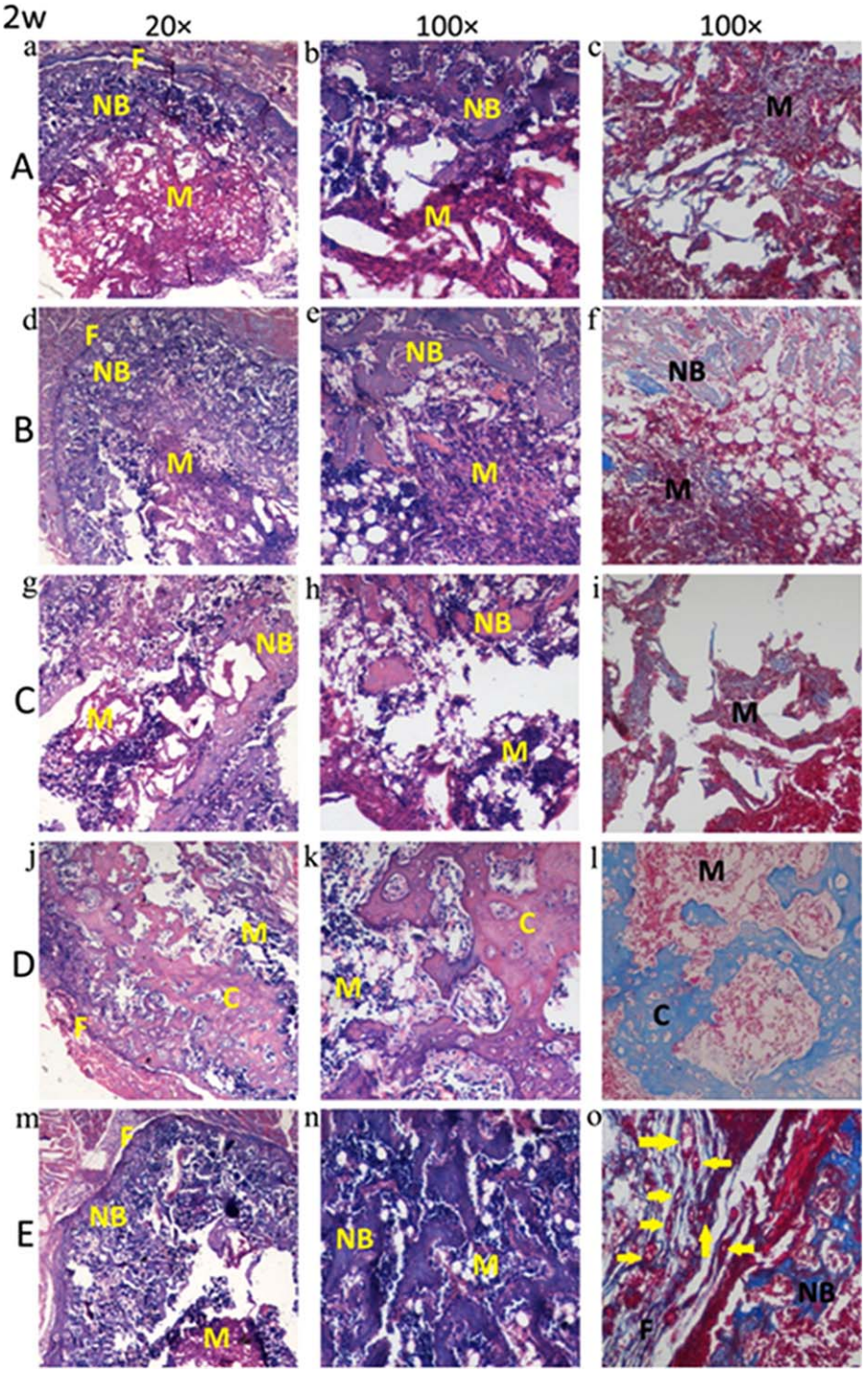

Figure 8. HE staining (left and middle columns) and Masson's trichrome staining (right column) of scaffolds implanted into rat hind limb muscle for 2 weeks. Original magnification: left column 20×; middle and right columns 100×. F: fibrous tissue; M: material; NB: new bone; C: Cartilage; Yellow arrows: blood vessels. [Color figure can be viewed in the online issue, which is available at wileyonlinelibrary.com.]

For group D, cartilage was observed at the 2nd week in Figure 8(j–l). Dense trabeculae and undegraded materials were seen at the 4th week in Figure 9(k). Mature trabeculae could be found in material areas in Figure 9(l). For group E, dense but not quite mature trabeculae was observed in Figure 8(m,n) at the 2nd week and mature trabeculae were seen in Figure 9(n) at the 4th week. Pleasantly surprised, abundant vessels were found in Figure 8(o) and Figure 9(o) both at the 2nd and 4th week, they would supply more nutrition for newly formed bone.

To our knowledge, better controlled release for BMP-2 is expected to obtain a better bone formation. Uncoated (group A, B, and C) and HPMC-coated (group E) scaffolds followed this regular pattern. Whereas, the osteogenesis of CMC-coated scaffolds was unexpectedly second to that of HPMC coated

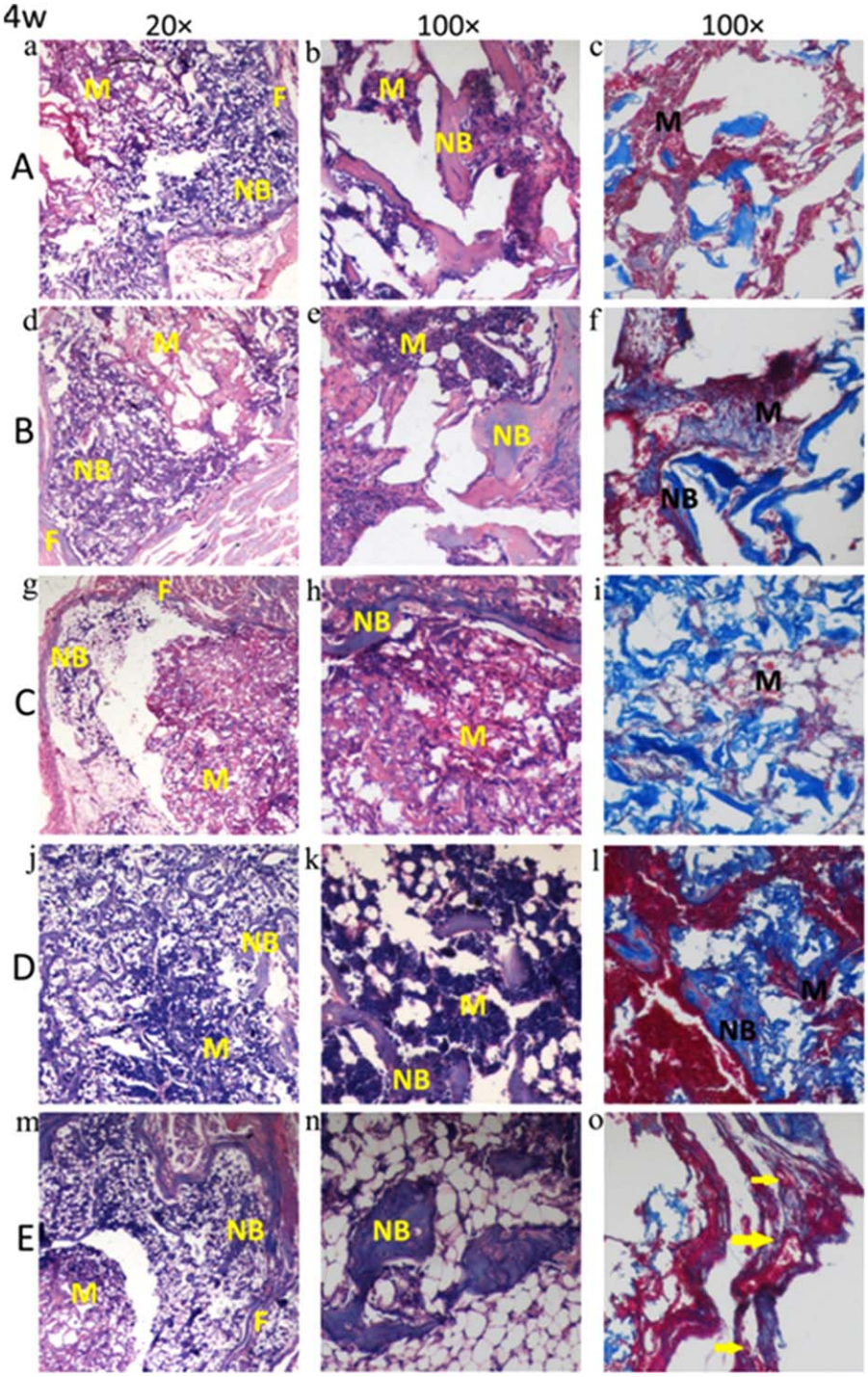

Figure 9. HE staining (left and middle columns) and Masson's trichrome staining (right column) of scaffolds implanted into rat hind limb muscle for 4 weeks. Original magnification: left column 20×; middle and right columns 100×. F: fibrous tissue; M: material; NB: new bone; Yellow arrows: blood vessels. [Color figure can be viewed in the online issue, which is available at wileyonlinelibrary.com.]

ones. This result indicated that too fast or too slow release rate for BMP-2 were not either suitable for homogeneous bone regeneration. According to description of Subha N. Rath,[2] the chemotactic factors induce migration of osteo-progenitor cells to the local site followed by induction of differentiation towards bone lineage and secretion of bone matrix proteins by bone-inducing growth factors, especially BMP-2. However, when BMP-2 is released into the blood stream and loses its bioactivity within hours after rapid degradation, the bone induction capacity may be not effective.[2,27] Therefore, if BMP-2 release rate is too fast, its quick clearance at local site would not benefit migration of osteo-progenitor cells, and it might induce an insufficient ectopic bone formation. To a certain extent, this may explain the differences in osteogenesis of uncoated (group

A, B and C) and HPMC- (group E) coated scaffolds. Whereas, due to the slowest rate for rhBMP-2 releasing from the CMC-coated scaffolds, in all probability cellular receptors of rhBMP-2 cannot capture enough available rhBMP-2 at the optimal stage of ossification, which leads to slightly inferior of osteogenesis compared to those HPMC-coated scaffolds with moderate release rate for rhBMP-2. However, CMC coating reduces the initial loss of rhBMP-2 and CMC-coated scaffolds possess better osteogenesis than uncoated scaffolds.

Besides the influence of release rate, the performance of HPMC itself might benefit bone tissue engineering. As abundant blood vessels were observed in Figures 8 and 9 both at the 2nd and the 4th week only for HPMC-coated scaffolds, more nutritions transmitted by vessels might facilitate the growth of newly formed bone, this consolidated its first place of osteogenesis in this article. It was reported that heparin-analogous polysaccharides possess a stimulatory effect on osteogenic activity of BMP-2.[28] Dextran-based polysaccharides could prolong the half-life of BMP-2 and promote its biological activity was also reported in Marie-Christelle Degat's research.[29] So the improvement of osteogenesis along with HPMC might attribute to not only the lower release rate but also a stimulatory effect on BMP-2 possessed by HPMC. We could make assumptions that as a kind of polysaccharide, HPMC may protect BMP-2 from proteolytic degradation or stimulate corresponding cellular growth factor receptors. And maybe there is a synergistic effect of HPMC with BMP-2 for vascularization. All of the hypotheses deserve further study.

CONCLUSION

In this study, we demonstrated that pliable and strong scaffolds could be obtained by modulating PDLLA/PCL ratios due to their complementary mechanical properties. Incorporation of β-TCP not only enhanced the strength but also improved the hydrophilicity of the complex scaffolds. The pore size ranged from 200 to 500 μm of scaffolds met the minimum requirement as a bone scaffolds and the porosity was above 80%. Besides, both CMC and HPMC coatings enhanced the mechanical properties and wettabilities of PDLLA/PCL/β-TCP scaffolds. Though the reduction in porosity was remarkable, the original porosity could be regained along with the dissolution of HPMC and CMC. Both coatings improved the osteoginsis of BMP-2-loaded scaffolds and HPMC had a better performance. Although the moderate release rate explained the well performed osteogenesis of BMP-2-loaded scaffolds along with HPMC coating, a deeper research should be done to figure out whether HPMC possesses a stimulatory effect on osteogenic activity of BMP-2.

Above all, porous PDLLA/PCL/β-TCP scaffolds along with HPMC coating as BMP-2 vehicles are promising candidates for application in bone repairing.

ACKNOWLEDGMENTS

The authors are indebted to the financial support from the National Basic Research Program of China (973 Program, 2012CB933600), the National Natural Science Foundation of China (No. 31271011), the National Science and Technology Support Program (2012BAI17B02), and the Program for New Century Excellent Talents in University (NCET-12–0856).

REFERENCES

1. Pneumaticos, S. G.; Triantafyllopoulos, G. K.; Basdra, E. K.; Papavassiliou, A. G. *J. Cell. Mol. Med.* **2010**, *14*, 2561.
2. Bhakta, G.; Rai, B.; Lim, Z. X. H.; Hui, J. H.; Stein, G. S.; Wijnen, A. J. V.; Nurcombe, V.; Prestwich, G.D.; Cool, S.M. *Biomaterials* **2012**, *33*, 6113.
3. Govender, S.; Csimma, C.; Genant, H. K.; Valentin-Opran, A.; Amit, Y.; Arbel, R.; Aro, H.; Atar, D.; Bishay, M.; Borner, M. G.; Chiron, P.; Choong, P.; Cinats, J.; Courtenay, B.; Feibel, R.; Geulette, B.; Gravel, C.; Haas, N.; Raschke, M.; Hammacher, E.; Velde, D. V. D.; Hardy, P.; Holt, M.; C. Josten,; Ketterl, R.L.; Lindeque, B.; Lob, G.; Mathevon, H.; McCoy, G.; Marsh, D.; Miller, R.; Munting, E.; Oevre, S.; Nordsletten, L.; Patel, A.; Pohl, A.; Rennie, W.; Reynders, P.; Rommens, P. M.; Rondia, J.; Rossouw, W. C.; Daneel, P. J.; Ruff, S.; Rüter, A.; Santavirta, S.; Schildhauer, T. A.; Gekle, C.; Schnettler, R.; Segal, D.; Seiler, H.; Snowdowne, R. B.; Stapert, J.; Taglang, G.; Verdonk, R.; Vogels, L.; Weckbach, A.; Wentzensen, A.; Wisniewski, T. *J. Bone Joint Surg. Am.* **2002**, *84*, 2123.
4. Chen, B.; Lin, H.; Wang, J. H.; Zhao, Y. N.; Wang, B.; Zhao, W. X.; Sun, W. J.; Dai, J.W. *Biomaterials* **2007**, *28*, 1027.
5. Watering, F. C. J.; Beucken, J. J. J. P.; Woning, S. P.; Briest, A.; Eek, A.; Qureshi, H.; Winnubst, L.; Boerman, O. C.; Jansen, J. A. *J. Control Release* **2012**, *159*, 69.
6. Eguchi, Y.; Wakitani, S.; Naka, Y.; Nakamura, H.; Takaoka, K. *J. Orthop. Res.* **2011**, *29*, 452.
7. Ruhe, P. Q.; Boerman, O. C.; Russel, F. G. M.; Mikos, A. G.; Spauwen, P. H. M.; Jansen, J. A. *J. Mater. Sci. Mater. Med.* **2006**, *17*, 919.
8. Chen, L.; Tang, C. Y.; Chen, D. Z.; Wong, C. T.; Tsui, C. P. *Comp. Sci. Tech.* **2011**, *71*, 1842.
9. Gan, Z. H.; Yu, D.H.; Zhong, Z. Y.; Liang, Q. Z.; Jing, X. B. *Polymer* **1999**, *40*, 2859.
10. Li, B.; Yoshii, T.; Hafeman, A. E.; Nyman, J.S.; Wenke, J. C.; Guelcher, S. A. *Biomaterials* **2009**, *30*, 6768.
11. Lanzetta, V.; Laurienzo, P.; Maglio, G.; Malinconico, M.; Musto, P.; Schiattarella, I. *J. Mater. Chem.* **2007**, *17*, 4508.
12. Gaasbeek, R. D. A.; Toonen, H. G.; Heerwaarden, R. J. V.; Buma, P. *Biomaterials* **2005**, *26*, 6713.
13. Dong, J.; Uemura, T.; Shirasaki, Y.; Tateishi, T. *Biomaterials* **2002**, *23*, 4493.
14. Leeuwen, A. C. V.; Bos, R. R. M.; Grijpma, D. W. *J. Biomed. Mater. Res. Part B: Appl. Biomater.* **2012**, *100B*, 1610.
15. Zerbo, I. R.; Bronckers, A. L. J. J.; Lange, G. L. D.; Burger, E. H.; Beek, G. J. V. *Clin. Oral. Implants Res.* **2001**, *12*, 379.
16. Yuan, H. P.; Bruijn, J. D. D.; Li, Y. B.; Feng, J. Q.; Yang, Z. J.; Groot, K. D.; Zhang, X. D. *J. Mater. Science: Mater. Med.* **2001**, *12*, 7.
17. Ragheb, A. A.; Nassar, S. H.; EI-Thalouth, I. A.; Ibrahim, M. A.; Shahin, A. A. *Carbohyd. Polym.* **2012**, *89*, 1044.

18. Melia, C. D. *Crit. Rev. Ther. Drug Carrier Syst.* **1991**, *8*, 395.
19. Zhang, L. F.; Sun, R.; Xu, L.; Du, J.; Xiong, Z. C.; Chen, H. C.; Xiong, C. D. *Mater. Sci. Eng. C* **2008**, *28*, 141.
20. Li, R. H.; Wozney J. M. *Trends Biotechnol.* **2001**, *19*, 255.
21. Broz1, M. E.; VanderHart, D. L.; Washburn, N. R. *Biomaterials* **2003**, *24*, 4181.
22. Newman, D.; Laredo, E.; Bello, A.; Grillo, A.; Feijoo, J. L.; Muller, A. J. *Macromolecules* **2009**, *42*, 5219.
23. Karageorgiou, V.; Kaplan, D. *Biomaterials* **2005**, *26*, 5474.
24. Brown, K. V.; Li, B.; Guda, T.; Perrien, D. S.; Guelcher, S. A.; Wenke, J. C. *Tissue Eng. Part A* **2011**, *17*, 1735.
25. Arafat, M. T.; Lam, C. X. F.; Ekaputra, A. K.; Wong, S. Y.; Li, X.; Gibson, I. *Acta Biomater.* **2011**, *7*, 809.
26. Velasco, M. V.; Ford, J. L.; Rowe, P.; Rajabi-Siahboomi, A. R. *J. Control Release* **1999**, *57*, 75.
27. Yamamoto, M.; Takahashi, Y.; Tabata, Y. *Biomaterials* **2003**, *24*, 4375.
28. Peschel, D.; Zhang, K.; Fischer, S.; Groth, T. *Acta Biomater.* **2012**, *8*, 183.
29. Degat, M.; Dubreucq, G.; Meunier, A.; Dahri-Correia, L.; Sedel, L.; Petite, H.; Logeart-Avramoglou, D. *J. Biomed. Mater. Res.* **2009**, *88A*, 174.